Colloid-facilitated tracer transport by steady random ground-water flow

V. Cvetkovic[a)]
Division of Water Resources Engineering, Royal Institute of Technology, Stockholm, Sweden

(Received 28 October 1999; accepted 5 June 2000)

We study the transport of reactive solute in a three-phase system (water–solid matrix-colloids) in natural porous media. Semianalytical (integral) solutions are derived for the first time, which can be used for computing expected concentration, mass flux, or discharge for the dissolved as well as for colloid-bounded tracer. The results are based on a few simplifying assumptions: advection-dominated transport, linear mass transfer reactions, and steady-state colloidal concentration. Derived semianalytical expressions capture the main features of colloid-facilitated transport (the reversible-equilibrium and irreversible-kinetic sorption of tracers on colloids), and are applicable for the general class of linear sorption processes on the porous matrix. Derived solutions account for spatial variability of flow *and* sorption parameters, which is relevant for field-scale applications. We apply the theoretical results to the transport of neptunium and plutonium, using flow and transport data from the alluvial aquifer near Yucca Mountain, Nevada. Based on the zeroth and first temporal moment, dimensionless indicators are proposed for assessing the potential impact of colloid-facilitated tracer transport in aquifers. Generic sensitivity curves show the importance of tracer-colloid kinetic rates. Even very low irreversible rates (which will generally be difficult to determine in the laboratory) may yield observable effects for sufficiently long transport times. The obtained results can be used for assessing the significance of colloid-facilitated tracer transport under field conditions, as well as for setting further constraints on relevant parameters which need to be estimated in the field. [S1070-6631(00)50509-1]

I. INTRODUCTION

Many contaminants in ground-water strongly interact with the immobile porous matrix, which retards their movement relative to ground-water flow. Colloidal particles of different origin (biocolloids, aluminosilicate clay minerals, organic colloids) are very often present in ground-water. These particles have a relatively small size and large specific surface area. The strong affinity of pollutants to interact with the immobile porous matrix, implies their strong affinity to interact with mobile colloidal particles as well. The binding of tracers to colloids may enhance their mobility in ground-water significantly, relative to the case where colloids are not present; this is likely to be relevant for a variety of pollutants.[1]

A class of pollutants for which colloid-facilitated transport may be of particular significance are radioactive isotopes. One reason why geological media is considered suitable for final disposal of spent nuclear fuel, is the strong affinity of many radionuclides to adsorb onto the porous matrix. The common view is that radionuclides accidentally released, would be contained in the geological media by adsorption, until sufficient decay has taken place. However, the presence of colloids may enhance radionuclide mobility in the ground-water, and reduce the efficiency of geological media to act as a natural barrier. Although these issues are of concern for safety and performance assessments of planned nuclear waste repositories, a modeling framework for evaluating the potential significance of field-scale tracer transport enhanced by colloids in heterogeneous geological media, is currently lacking.

Wider interest in understanding colloid-facilitated contaminant migration on the field-scale, followed the discovery of plutonium in a deep aquifer at the Nevada test site, significantly further downstream than had been predicted based on its sorption properties and the mean ground-water flow (e.g., Ref. 2). The discovered plutonium was associated with inorganic colloidal particles,[2] suggesting that it was carried by these with approximately the ground-water velocity.[2,3] A similar observation was made earlier in a shallow aquifer for plutonium and americium,[4] although this finding has been questioned more recently.[5]

Two main problems in aquifers are inaccessibility and random spatial variability in physical and chemical properties. In practice, a limited number of field measurements is usually available for characterizing flow and reaction parameters, and contaminant transport can in most cases be monitored at only few locations. Thus the challenge in predicting the fate of contaminants in ground-water is on the one hand to account for coupled flow and reaction processes under conditions of heterogeneity, and on the other hand to provide statistical descriptions based on information which can realistically be extracted from the subsurface.

Current models for colloid-facilitated tracer transport are based on a one-dimensional convection–diffusion equation with constant parameters, and are suitable for the laboratory scale ($<10^{-1}$ m) (e.g., Refs. 6–8). Modeling colloid-facilitated tracer migration on the field scale ($>10^{2}$ m),

a)Electronic mail: vdc@wre.kth.se

however, is still a major challenge in view of the random, three-dimensional spatial variability of subsurface properties.[9]

In this work, we present for the first time a Lagrangian probabilistic model for colloid-facilitated tracer migration in heterogeneous aquifers, which accounts for the random spatial variability in physical *and* reaction properties. Our general Lagrangian methodology developed in the past for reactive transport in a two-phase system (fluid–solid matrix)[10–13] is here extended to a three-phase system (fluid–solid matrix-colloids). We provide solutions of the transport problem in the form of semianalytical (integral) expressions, and illustrate the potential significance of colloid-facilitated tracer transport for plutonium and neptunium using flow and transport data for the alluvial aquifer near Yucca Mountain, Nevada.

II. PROBLEM DESCRIPTION AND ASSUMPTIONS

Ground-water flows in an aquifer with a steady-state, spatially varying random velocity, $\mathbf{V}(\mathbf{x})$ where $\mathbf{V}(V_1, V_2, V_3)$ and $\mathbf{x}(x_1, x_2, x_3)$ (see Appendix A for a brief summary on ground-water flow in heterogeneous aquifers). A dissolved contaminant is injected into the aquifer over an injection area [Fig. 1(a)], the typical scale of which is either large, or small, relative to the transverse integral scale of aquifer heterogeneity. Alternative interpretations of the probabilistic solutions of the transport problem depending on the size of the injection area, are discussed in Sec. V.

If the ground-water contains colloidal particles (as often is the case), these can bind part of the contaminant mass. Both the colloids and contaminants are in general subject to mass transfer/transformation processes, due to various physico–chemical interactions, such as chemical sorption–desorption (e.g., ion-exchange, surface complexation), deposition/filtration, decay/degradation, etc.

The problem of tracer-facilitated tracer transport arises due to two parallel processes: on the one hand, the colloids move essentially with ground-water velocity; on the other hand, part of the tracer mass attaches (''sorbs'') onto the colloids, i.e., there is transfer of tracer mass from the solution (dissolved tracer) onto the *mobile* particulate matter (colloids). The result is that tracer retention due to sorption onto the *immobile* porous matrix is reduced, and tracer mobility is enhanced, relative to the case where colloids are not present [Fig. 1(a)]. We wish to provide here a model for colloid-facilitated tracer transport which accounts for aquifer heterogeneity in flow and reaction parameters, and captures the most dominant mass transfer reactions.

It is well established that for computing average transport quantities in the subsurface (e.g., expected tracer concentration or discharge, spatial and temporal moments), the random flow velocity controls physical transport on the field scale (e.g., Refs. 14, 15). In other words, dispersion due to velocity fluctuations on the pore scale is negligible compared to the field scale dispersion due to fluctuations of $\mathbf{V}$. This is the basis for our first assumption (this assumption is analogous to neglecting molecular diffusion in turbulent diffusion):

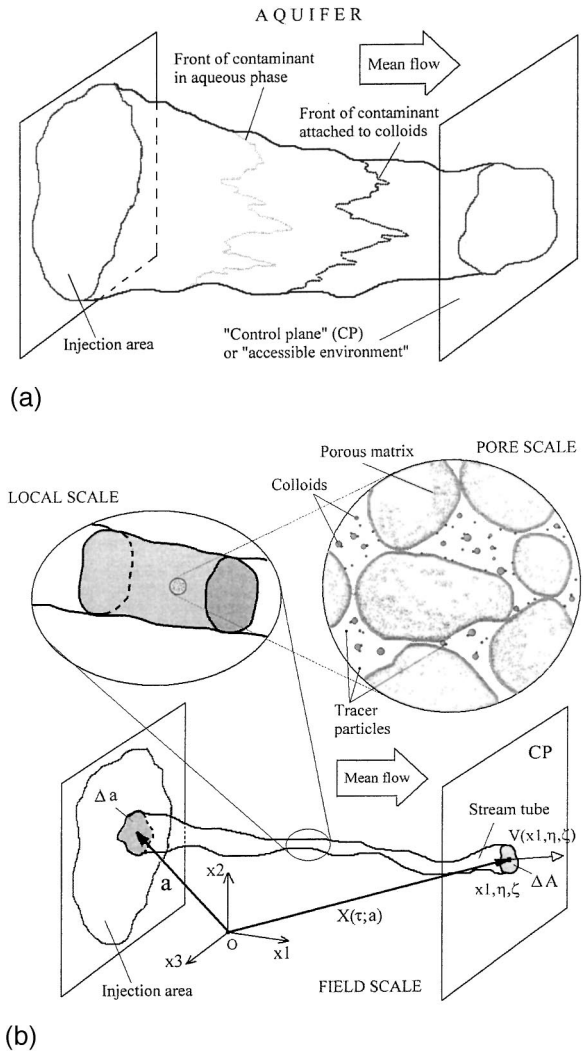

FIG. 1. Configuration sketches of (a) the colloid-facilitated tracer transport problem on the field scale; (b) a random streamtube originating at **a** and extending through an aquifer to the control plane (CP) at x_1. The mean ground-water flow is set parallel with the x_1-axis. Three distinct scales in (b) are *field scale* ($\gtrapprox 10^2$ m) determined by the scale of the transport problem (from $x_1=0$ to x_1), the *local scale* (or laboratory scale) ($\approx 10^{-1}-10^0$ m) on which the support volume/area for all quantities and parameters is defined, and *pore scale* ($<10^{-3}$ m).

(i) physical transport is advection-dominated, i.e., pore-scale dispersion can be neglected.

The support volume for the ground-water velocity is defined on the local scale, $\approx 10^{-1}-10^0$ m [see Fig. 1(b)]. A mean flow exists and without loss of generality, we align the x_1-axis with the mean flow direction such that $\langle V_1 \rangle \equiv U$, $\langle V_2 \rangle = \langle V_3 \rangle = 0$, with $\langle\ \rangle$ being the ensemble average operator (Fig. 1).

For advective transport, a streamtube is defined by streamlines emerging from an elementary area Δa in the vicinity of $\mathbf{x}=\mathbf{a}(0, a_2, a_3)$ [Fig. 1(b)]. We study the transport of a dissolved tracer released over Δa into the aquifer at time $t=0$. At $t>0$, the tracer migrates toward the ''control plane'' (CP) (also referred to as the ''accessible environment'') at x_1 [Figs. 1(a) and 1(b)].

In natural systems colloids are always present in ground-

water. If the concentration of colloids does not increase substantially with the tracer release, then it is realistic to suppose that an equilibrium state for the colloidal concentration at the time of tracer release has been established. In recent laboratory experiments designed to mimic field conditions, for instance, actinides were injected as tracers in a column only after the colloidal concentration attained a steady-state value.[8] In cases where substantial amounts of colloids are injected with a strongly or moderately sorbing tracer, colloidal concentration is likely to reach a steady-state over short times relative to the tracer transport time. For instance, concentration of kaolinite particles ($<2\ \mu$m) injected in a sand column simultaneously with cesium, reached a steady-state after less than 2% of the transport time.[7]

The second assumption of our analysis is:

(ii) colloidal concentration is a function of space only, i.e., steady-state conditions are applicable over the considered space-time domain.

For most applications, contaminants in ground-water are present at low concentrations, hence, the wide class of linear mass transfer models is sufficient (e.g., Refs. 16, 6). We state our third assumption as:

(iii) all mass transfer reactions for the tracer are linear.

III. THREE-PHASE TRANSPORT MODEL

In this section, we develop a transport model in several steps. First, we provide a solution for advective, steady-state transport of colloids, and then establish Eulerian and Lagrangian mass balance equations for the tracer. Finally, we adopt a few alternative mass transfer (sorption) models for tracer exchange between the three phases in which the spatially variable colloidal concentration is a parameter.

The assumption of advection-dominated transport implies that the mass flux vectors for the colloids and tracer are respectively

$$\mathbf{J}_c(\mathbf{x},t)\equiv\vartheta C_c(\mathbf{x},t)\mathbf{V}(\mathbf{x}),\quad \mathbf{J}(\mathbf{x},t)\equiv\vartheta C(\mathbf{x},t)\mathbf{V}(\mathbf{x}),\qquad (1)$$

where C_c $[\mathrm{ML}^{-3}]$ is the colloidal and C $[\mathrm{ML}^{-3}]$ the tracer concentration defined per unit volume of fluid, and ϑ is the porosity that is assumed constant; the support volume for both C_c and C is defined on the local scale [Fig. 1(b)].

The advection velocities for colloids and tracer are in (1) set equal, since we consider sufficiently small colloidal particles (irrespective of their origin), as to be dynamically inert.[6,7] In reality, the advection velocity of the colloids is somewhat larger than that of an inert tracer due to ''exclusion'' phenomena, however, this effect has been neglected on the laboratory scale (e.g., Refs. 7, 8) and is anticipated even less relevant for the field scale. [The effect of ''exclusion'' can be incorporated into the analysis either as a spatially uniform or variable factor that multiplies $\mathbf{V}$ in the expression (1) for $\mathbf{J}_c$.]

A. Colloids

Exchange processes of interest for colloidal transport are *removal* due to e.g., filtration, and *generation*. Laboratory evidence indicates that colloidal removal in porous media can be described as first-order linear loss,[6,7,9] and that filtration models may be applicable.[17] Generation of colloids is more difficult to quantify, both in the field and the laboratory. In fact, little is known about colloidal removal and generation on the field-scale.[17,18,3] It is apparent, however, that physical as well as chemical factors may influence generation and deposition of colloids.[17,18]

We propose here a steady-state model for colloidal transport in the form

$$\nabla\cdot(\mathbf{V}C_c)=-\epsilon(\mathbf{x})C_c+\chi(\mathbf{x}),\qquad (2)$$

where $C_c=C_c^0$ at $\mathbf{x}=\mathbf{a}$, and $\epsilon(\mathbf{x})\geqslant 0$ is the irreversible deposition/removal rate. ϵ $[\mathrm{T}^{-1}]$ is likely to be correlated to the magnitude of the flow velocity, $V(\equiv|\mathbf{V}|)$. In fact, a common assumption for deposition (filtration) under laboratory conditions is $\epsilon\sim V$ (e.g., Refs. 19, 9). The parameter $\chi(\mathbf{x})$ $[\mathrm{ML}^{-3}\ \mathrm{T}^{-1}]$ (defined per unit volume of fluid), quantifies the generation of colloids; in general, χ varies along a trajectory, due to spatial variability in the controlling physicochemical properties.

The three-dimensional Eulerian Eq. (2) can be transformed onto a trajectory (stream tube) using Lagrangian coordinates (τ,η,ζ) [see Appendix A and Fig. 1(b)]; the methodology was first presented in Ref. 10 (see also Ref. 12). The benefit of this transformation is that a three-dimensional Eulerian system is reduced to a one-dimensional Lagrangian system in the (t,τ) domain, where τ is random.

The result of transforming (2) is the Lagrangian equation

$$\frac{dC_c}{d\tau}=-\epsilon(\tau)C_c+\chi(\tau),\qquad (3)$$

where the Lagrangian counterpart of $\epsilon(\mathbf{x})$ is $\epsilon(\tau)=\epsilon[\mathbf{X}(\tau)]$ (see Appendix A). Similarly $C_c(\tau)$ in (3) is related to $C_c(\mathbf{x})$ in (2) as $C_c(\tau)=C_c[\mathbf{X}(\tau)]$; we retain the same notation for simplicity.

We solve (3) for C_c along a trajectory as

$$C_c(\tau)=e^{-\nu(\tau)}\left[\int_0^\tau\chi(\theta)e^{\nu(\theta)}d\theta+C_c^0\right],\quad \nu(\tau)=\int_0^\tau\epsilon d\tau'.\qquad (4)$$

If the generation of colloids is negligible, $C_c(\tau)=C_c^0\times\exp(-\nu)$.

The simplest case is if both the removal and generation are relatively small, such that $\epsilon=\chi=0$ at all points, and $C_c=C_c^0$ is uniform along the entire trajectory.

B. Tracer: Eulerian formulation

Let S $[\mathrm{MM}^{-1}]$ denote the concentration of a tracer on colloids, defined per unit colloidal concentration; the actual tracer concentration is then SC_c. Furthermore, let N $[\mathrm{ML}^{-3}]$ denote the concentration of tracer immobilized on the porous matrix by sorption, defined per unit bulk volume.

The Eulerian mass balance equations that link the four concentrations C_c, C, S, and N are written in a general form as

$$R\frac{\partial C}{\partial t}+\nabla\cdot(R_c C\mathbf{V})=\psi_c(C,S)+\psi_{\rm pm}(C,N),$$

$$\frac{\partial(C_c S)}{\partial t}+\nabla\cdot(C_c S\mathbf{V})=\psi_c'(C,S)-\epsilon C_c S, \tag{5}$$

$$\frac{\partial N}{\partial t}=\psi_{\rm pm}'(C,N),$$

where

$$R\equiv R_c+K_d,\quad R_c\equiv 1+K_c=1+\kappa C_c, \tag{6}$$

are referred to as retardation factors, and $C_c(\tau)$ is given in (4).

In (5)–(6), K_d is the dimensionless partitioning coefficient (or equilibrium constant) for equilibrium sorption sites on the porous matrix, K_c is the dimensionless partitioning coefficient for equilibrium sorption sites on the colloids, and κ is the dimensionless partitioning coefficient for equilibrium sorption sites on the colloids defined per unit concentration (or density) of colloids. Thus two types of sorption sites on the colloids, as well as on the porous matrix, are considered in (5)–(6): one where sorption is relatively fast (equilibrium), and one where it is relatively slow (kinetically controlled). With the formulation (5), we clearly distinguish equilibrium from kinetic sorption on both the colloids and the porous matrix: $\psi_c=\psi_c'=\psi_{\rm pm}=\psi_{\rm pm}'=0$ implies that only equilibrium sorption takes place.

As a consequence of the linearity assumption, the source/sink components ψ_c, ψ_c', $\psi_{\rm pm}$, $\psi_{\rm pm}'$ are linear in the tracer concentrations, i.e., $W\psi_{\rm pm}=\psi_{\rm pm}(WC,WN)$, etc..., where W is independent of C, N, S.

C. Tracer: Lagrangian formulation

The Eulerian equation system (5) can be transformed onto a trajectory similar to (3) (see also Appendix A). The result is a Lagrangian equation system for the concentrations C, S, N in the one-dimensional (t,τ)-domain.

In many applications, tracer detection is such that we may require tracer mass flux, or discharge, across a specified control plane (CP) [Fig. 1(a)], rather than (or in addition to) the concentration. Furthermore, different injection modes are relevant in applications, i.e., different quantities may be specified at the injection point $\mathbf{x}=\mathbf{a}$, such as tracer concentration, discharge, or the mass flux.

The dissolved tracer mass flux vector is defined in (1) and we are particularly interested in its x_1-component, $J_1=\vartheta C V_1$. Dissolved tracer discharge, $X\,[\mathrm{M\,T^{-1}}]$, is obtained by integrating J_1 over the CP, i.e., $X\equiv\int J_1\,dx_2\,dx_3=qC$, where $q\,[\mathrm{L^3\,T^{-1}}]$ is the (constant) volumetric flow rate for a stream tube. The corresponding quantity for the colloid-bounded tracer is $Y\equiv\int J_{S1}dx_2\,dx_3=qSC_c$, where $J_{S1}=\vartheta SC_cV_1$. Note that the fluid continuity statement is $q=\vartheta\Delta a V_0=\vartheta\Delta A V_1=$const. in any given realization of an aquifer, where $V_0\equiv V_1(\mathbf{a})$ and ΔA is the cross-sectional area of the stream tube at the CP [see Fig. 1(b)].

It can be shown that for linear mass transfer reactions, the solution for all injection/detection modes for a stream tube involves what we refer to as the ''reaction function'';[10] the reaction function (''reaction function'' corresponds to what is also referred to as the ''impulse–response function'') quantifies how a pulse of unit strength at $\mathbf{x}=\mathbf{a}$ is ''deformed'' by mass transfer reactions, as a function of τ. In our particular case, two reaction functions are relevant: γ_X $[\mathrm{T^{-1}}]$ and γ_Y $[\mathrm{T^{-1}}]$. γ_X, for instance, is most conveniently defined in the Laplace domain as

$$\hat{\gamma}_X\equiv\frac{\hat{C}}{\hat{C}_0}=\frac{\hat{X}}{\hat{X}_0}=\frac{\hat{J}_1}{\hat{J}_{10}},$$

where $C_0(t)\equiv C(t,0)$, $X_0(t)\equiv X(t,0)$, and $J_{10}(t)\equiv J_1(t,0)$ denote the time change of dissolved tracer concentration, discharge, and mass flux, respectively, at $\mathbf{x}=\mathbf{a}$, i.e., for $\tau=0$.

A case of common interest is the injection of a specified contaminant mass, ΔM, into an aquifer at a given location and rate; the special case is instantaneous injection. The boundary conditions are

$$C_0(t)=\frac{\Delta M}{q}\phi(t),\quad X_0(t)=\Delta M\phi(t),$$
$$J_{10}(t)=\Delta M\,\delta(x_2-\eta)\,\delta(x_3-\zeta)\,\phi(t), \tag{7}$$

where $\phi(t)$ $[\mathrm{T^{-1}}]$ is the specified release rate, and η,ζ are the Lagrangian transverse coordinates of the trajectory crossing the CP [Appendix A, Fig. 1(b)], with $\eta=a_2,\zeta=a_3$ for $\mathbf{x}=\mathbf{a}$, $\tau=0$. Note that $\delta(x_2-\eta)\,\delta(x_3-\zeta)=1/\Delta A$ and $\Delta A=\Delta a$ for $\mathbf{x}=\mathbf{a}$, $\tau=0$. For pulse injection, $\phi(t)=\delta(t)$, and the solution for C, X, J_1 is equal to γ_X multiplied by a constant with respect to t,τ. Relationships similar to (7) can also be written for the colloid-bounded tracer.

The Lagrangian mass balance equations for the tracer are now written in terms of the reaction functions γ_X and γ_Y, as

$$R'\frac{\partial\gamma_X}{\partial t}+\frac{\partial\gamma_X}{\partial\tau}=\frac{1}{R_c}\psi_c(\gamma_X,\gamma_Y)+\frac{1}{R_c}\psi_{\rm pm}(\gamma_X,N_X)-\frac{d\ln R_c}{d\tau}\gamma_X,$$

$$\frac{\partial\gamma_Y}{\partial t}+\frac{\partial\gamma_Y}{\partial\tau}=\psi_c'(\gamma_X,\gamma_Y)-\epsilon\gamma_Y, \tag{8}$$

$$\frac{\partial N_X}{\partial t}=\psi_{\rm pm}'(\gamma_X,N_X),$$

where

$$R'\equiv\frac{R}{R_c}=1+K_d',\quad K_d'\equiv\frac{K_d}{R_c}. \tag{9}$$

In (8), N_X $[\mathrm{MT^{-1}}]$ is an auxiliary quantity, proportional to the immobilized tracer concentration, N. The three-dimensional nature of the solutions γ_X and γ_Y is preserved through their dependence on $\mathbf{a}$ and τ (A1). Also, we require the computation of η,ζ in order to map C, S, J_1, or J_{S1} onto the CP (see Appendix A).

Tracer mass balance between the three phases is ensured by the following relationships:

$$\psi_{\rm pm}'=-\frac{1}{R_c}\psi_{\rm pm},\quad \psi_c'=-\frac{1}{R_c}\psi_c,$$

which is apparent in the case where colloidal concentration is uniform, with $\epsilon=\chi=0$ and $R_c=\text{const}$. For $K_c\neq 0$, part of the tracer mass is bounded on colloids by equilibrium sorption, where $R_c>1$. Because the tracer is injected in the aqueous phase, the mass transfer rates (i.e., ψ's) are scaled (decreased) by a factor R_c to account for the fact that at any given time, only the tracer mass present in the aqueous phase is available for exchanges with the matrix and/or kinetic exchanges with colloids. If equilibrium sorption on colloids is not present (or is neglected), then $R_c=1$.

The next step in the model formulation is the specification of the sink/source terms ψ_{pm} and ψ_c, which characterize sorption processes. (In this study, ''sorption'' refers to the exchange of the tracer mass between the aqueous phase and colloids, as well as between the aqueous phase and the porous matrix, irrespective of the actual detailed mechanism involved. In reality, several exchange mechanisms will be simultaneously ''active'' within the support volume on the local scale [Fig. 1(b)]; these will generally be indistinguishable and therefore are described by lumped mass transfer (or sorption) parameters, separately for sorption onto colloids, and for sorption onto the porous matrix.)

D. Sorption on porous media

Different physical and chemical mechanisms contribute to the binding of tracers onto the porous matrix. Chemical sorption (e.g., ion-exchange, surface complexation) is relatively rapid and can be well described as instantaneous (equilibrium); tracer transport which is dominated by equilibrium sorption is referred to as ''ideal.''[16,20] As a rule, kinetic effects are observed in tracer experiments from the laboratory to the field scale, which is attributed to physical sorption, e.g., due to intra-aggregate diffusion, or diffusion into immobile water;[20,21] transport where mass transfer exhibits kinetic effects is referred to as ''nonideal.''[16,20]

The general class of linear mass transfer models for porous media (first-order with single or multiple rates, diffusion in aggregates of different geometry, etc.), is most conveniently expressed in the Laplace domain as (e.g., Refs. 22, 10, 12)

$$\frac{\hat{N}_X}{\hat{\gamma}_X}=\mathcal{F}\{s,\mathcal{P}[\mathbf{X}(\tau;\mathbf{a}]\}, \tag{10}$$

where $\hat{}$ denotes the Laplace transform, s is the Laplace transform variable, $\mathcal{P}(\mathbf{x})$ is the vector of mass transfer parameters [including $R_c(\tau)$], and $\mathbf{X}$ is the equation of the random trajectory originating at $\mathbf{a}$ (see Appendix A). Thus $\mathcal{F}$ provides an implicit definition of ψ_{pm} in the Laplace domain. Note that $\psi_{\text{pm}}=0$ (''ideal'' transport) implies $\mathcal{F}=0$ or $\mathcal{F}\sim s$; in the following, ''ideal'' transport will imply $\mathcal{F}=0$ for simplicity.

E. Sorption on colloids

Comparatively little experimental data is available for tracer sorption onto colloids, in particular on the field scale. It is known that a wide range of mechanisms may lead to tracer sorption onto colloids, depending on tracer properties, and on colloidal origin and composition.[1] For instance, organic materials such as humic and biopolymeric substances, bind hydrophobic organic contaminants, metal ions, and actinides. Furthermore, inorganic substances such as layer silicate clays and calcium carbonate, as well as surfaces of iron, manganese, aluminum, and silicate oxide particles adsorb both metals and organic contaminants.

An important experimentally established fact is that tracers sorb onto colloids; this sorption is both reversible and irreversible (e.g., Refs. 4, 7). A fairly general model for tracer mass transfer between the aqueous and particulate phase is the ''bi-linear,'' or kinetic Langmuir model, which accounts for the fact that a number of binding sites on colloids may be limited.[23] If the tracer concentrations are sufficiently low relative to the colloidal concentration in a control volume, then the kinetic Langmuir model can be linearized (e.g., Refs. 6, 7).

In this analysis, we consider low contaminant concentrations, and postulate the linear model for tracer sorption onto colloids $\psi_c\equiv-\alpha_f C+\alpha_r C_c S$ (e.g., Refs. 6, 7), here adopted as

$$\psi_c\equiv-\alpha_f\gamma_X+\alpha_r\gamma_Y. \tag{11}$$

In (11), α's are rates for tracer exchange between solution and kinetic sites on colloids: α_f denotes the ''forward'' rate, and α_r the ''reverse'' rate. The forward rate is dependent on the colloidal concentration C_c, and linear dependence is a common assumption (see, e.g., Ref. 23). A special case of interest is irreversible sorption (that may take place simultaneously with equilibrium sorption), which is obtained in the limit $\alpha_f/\alpha_r\to\infty$, and $\alpha_r\to 0$.

IV. SOLUTIONS FOR A TRAJECTORY

We shall solve (8)–(10) for equilibrium ($\psi_c=0$) and irreversible sorption on colloids ($\alpha_r=0$), each case for ''ideal'' (formally obtained for $\psi_{\text{pm}}=\mathcal{F}=0$) and ''nonideal'' transport (i.e., $\mathcal{F}\neq 0$ and $\mathcal{F}$ is not a linear function of s). These combinations cover a wide range of cases relevant for applications. For simplicity, we seek solutions only for the case where a tracer is injected in the solution, i.e., $\gamma_X(t,0)=\delta(t)$, $\gamma_Y(t,0)=0$, and the domain is initially tracer-free, i.e., $\gamma_X(0,t)=\gamma_Y(0,t)=0$. In the absence of mass transfer reactions, a unit pulse is preserved as a pulse, whereby $\gamma_X=\delta(t-\tau)$ and $\gamma_Y=0$.

In (8)–(10), all the mass transfer parameters can vary spatially. The equations are considerably simplified if we assume mass transfer parameters (including the colloidal concentration) to be spatially uniform; in Appendix C, we provide analytical solutions for this case.

A. Equilibrium sorption on colloids

If kinetic sites on colloids have a negligible effect on tracer transport, then $\psi_c=0$ and the tracer is sorbed only on the equilibrium sites on colloids (i.e., $S=Y=0$). In such a case, the governing transport equations are

$$R'\frac{\partial \gamma_X}{\partial t}+\frac{\partial \gamma_X}{\partial \tau}=\frac{1}{R_C}\psi_{\rm pm}(\gamma_X,n_X)-\frac{d\ln R_C}{d\tau}\gamma_X,$$
$$\frac{\partial N_X}{\partial t}=-\frac{1}{R_c}\psi_{\rm pm}(\gamma_X,N_X). \tag{12}$$

Equations (12) can be solved in the Laplace domain to yield

$$\hat{\gamma}_X=\exp\left\{-s(\tau+\mu)-\int_0^\tau \mathcal{F}[s,\mathcal{P}(\theta)]d\theta-\varsigma\right\}, \tag{13}$$

where

$$\mu(\tau)\equiv\int_0^\tau (R'-1)d\theta=\int_0^\tau \frac{K_d(\theta)}{[1+K_c(\theta)]}d\theta,$$
$$\varsigma(\tau)\equiv\ln(R_c/R_c^0), \tag{14}$$

with $K_c=\kappa C_c$, $C_c(\tau)$ is given in (4), and $R_c^0\equiv R_c(0)$ at $\mathbf{x}=\mathbf{a}$. The parameter vector $\mathcal{P}$ in (13) follows a trajectory (see Appendix A), and incorporates the parameter R_c in (6).

Inversion of (13) yields the general solution for ''non-ideal'' transport

$$\gamma_X(t,\tau)=e^{-\varsigma}\gamma(t-\mu,\tau), \tag{15}$$

where

$$\gamma(t,\tau)=\mathcal{L}^{-1}\left\{\exp\left[-s\tau-\int_0^\tau \mathcal{F}(s,\theta)d\theta\right]\right\}, \tag{16}$$

and $\mathcal{L}^{-1}$ denotes the inverse Laplace transform.

For ''ideal'' transport where tracer is sorbed onto the porous matrix under equilibrium conditions, $\psi_{\rm pm}=\mathcal{F}=0$ and $\gamma(t,\tau)\equiv\delta(t-\tau)$; we then get the general equilibrium solution from (15) as

$$\gamma_X(t,\tau)=\delta(t-\tau-\mu). \tag{17}$$

Equations (14) and (17) make apparent the effect of colloids on transport for the equilibrium case. If no colloids are present, or the sorption on colloids is negligible, $R_c=1$; (14) then yields $\mu=\int K_d d\theta$ and (17) is applicable to the case of equilibrium sorption on the porous matrix with a spatially variable partitioning coefficient.[12] For $K_c>0$ due to the presence of colloids, i.e., $R_c>1$, μ of (14) decreases whereby the transport is enhanced relative to the case where colloids are not present. Equilibrium sorption on colloids implies that part of the tracer mass is *always* residing on colloids, and hence is unavailable for sorption on the porous matrix; this in effect reduces the retardation due to sorption on the porous matrix. Equation (17) generalizes the simplest model used in applications (e.g., Ref. 17) to the case where sorption parameters are spatially variable. We emphasize, however, that the equilibrium sorption model cannot explain field observations on colloid-facilitated tracer transport (e.g., Ref. 17).

B. Irreversible sorption on colloids

For many applications (e.g., risk and safety assessment of contaminated sites, or repositories), the most interesting case is the (almost) irreversible binding of tracers to colloids. The combined field–laboratory study on colloid-facilitated transport,[4] for instance, suggests irreversible association of plutonium and americium with colloids in the size range of 25–450 nm.

In the following, we consider irreversible sorption on the kinetic sites, combined with reversible sorption on the equilibrium sites, of the colloids. Setting $\alpha_r=0$ and $\alpha(\mathbf{x})\equiv\alpha_f(\mathbf{x})/R_c$, the following coupled equation system is obtained from (8):

$$R'\frac{\partial \gamma_X}{\partial t}+\frac{\partial \gamma_X}{\partial \tau}=-\left(\alpha+\frac{d\ln R_c}{d\tau}\right)\gamma_X+\frac{1}{R_c}\psi_{\rm pm}(\gamma_X,N_X),$$
$$\frac{\partial \gamma_Y}{\partial t}+\frac{\partial \gamma_Y}{\partial \tau}=\alpha\gamma_X-\epsilon\gamma_Y, \tag{18}$$
$$\frac{\partial N_X}{\partial t}=-\frac{1}{R_c}\psi_{\rm pm}(\gamma_X,N_X).$$

The solution for the reaction functions is obtained from (18) in the Laplace domain as

$$\hat{\gamma}_X(s,\tau)=\exp\left[-s(\tau+\mu)-\int_0^\tau \mathcal{F}(s,\theta)\,d\theta-\omega-\varsigma\right],$$
$$\hat{\gamma}_Y(s,\tau)=e^{-\nu-s\tau}\int_0^\tau \alpha\exp\left[-s\mu-\int_0^\theta \mathcal{F}(s,\theta')d\theta'-\omega+\nu-\varsigma\right]d\theta, \tag{19}$$

where

$$\omega(\tau)\equiv\int_0^\tau \alpha(\theta)d\theta, \tag{20}$$

and μ and ν are defined in (14) and (4), respectively.

We invert $\hat{\gamma}_X$ in (19) to obtain

$$\gamma_X=e^{-\varsigma-\omega}\gamma(t-\mu,\tau), \tag{21}$$

where γ is defined in (16). Inversion of $\hat{\gamma}_Y$ in (19) yields

$$\gamma_Y=e^{-\nu}\int_0^\tau \alpha(\theta)e^{\nu-\omega-\varsigma}\gamma(t-\tau-\mu+\theta,\theta)d\theta, \tag{22}$$

where μ, ς, ν, ω in the integrand are functions of θ.

For ''ideal'' transport ($\mathcal{F}=0$), $\gamma=\delta(t-\tau)$, and we obtain

$$\gamma_X=e^{-\varsigma-\omega}\delta(t-\mu-\tau), \tag{23}$$

which generalizes our earlier result[12] to the case where the tracer is sorbed reversibly and irreversibly onto colloidal particles. For γ_Y, we get

$$\gamma_Y=e^{-\nu}\int_0^\tau \alpha(\theta)\,e^{\nu-\omega-\varsigma}\delta(t-\tau-\mu)d\theta, \tag{24}$$

where μ, ς, ν, ω in the integrand are functions of θ.

The Lagrangian random variable ω of (20) is an important new quantity derived in this study. It integrates the irreversible transfer of a tracer from the aqueous to the particulate phase (colloids), along a trajectory. Larger values of ω (obtained either due to increasing α or longer residence times along a trajectory) imply larger tracer mass transfer

from solution to colloids. α, and consequently ω, depend on the amount of colloids present in any given volume, analogous to the forward rate for reversible sorption (see Sec. III D). A simple linear model for this dependence is $\alpha = \alpha_0 C_c$, where α_0 [L^3MT^{-1}] may be referred to as an ''intrinsic'' irreversible rate, i.e., an irreversible rate per unit colloidal concentration.

Equations (21)–(22) summarize the most general solutions for a single trajectory obtained in this work. Out of the four random Lagrangian varibles μ, ς, ω, and ν, two are associated with equilibrium sorption (μ and ς), and two with kinetic mass transfer (ν and ω, either by colloidal removal/filtration, or irreversible tracer sorption on colloids). In (21)–(22) [and also (23)–(24)] we see two simultaneous irreversible mechanisms: the tracer is transferred from the aqueous solution to the colloids (with $\omega>0$), and then irreversibly removed from the system by filtration (with $\nu>0$). Thus the presence of colloids can both enhance as well as detract transport, depending on the ratio of the mass transfer parameters ν and ω. These two parameters are therefore critical when assessing the potential impact of colloid-facilitated tracer transport, as described by solutions (21)–(22). [Note that in (21)–(22) we consider removal and generation of colloids as separate mechanisms, such that the possibility of returning (i.e., being ''generated'') of once removed colloids with tracer attached, is negligible.]

Because the upper limit of the integrals in (19), (24), and (22) is random due to the randomness of the fluid velocity **V**, it is convenient to transform the integral from the τ-domain to x_1-domain (see Appendix A). For instance, we have for ''ideal'' transport ($\mathcal{F}=0$) from (19) in the x_1-domain

$$\hat{\gamma}_Y(s,x_1) = e^{-\nu(x_1)-s\tau}\int_0^{x_1}\left(\frac{\alpha}{V_1}\right) \times \exp\{-s\,\mu+\nu-\omega-\varsigma\}d\xi, \tag{25}$$

where α, V_1 are computed at the point where the trajectory originating at $\mathbf{x}=\mathbf{a}$ crosses the CP, and μ,ν,ς,ω in the integrand are functions of the integration variable ξ.

V. PROBABILISTIC SOLUTIONS

Due to the random spatial variability in the physico–chemical properties of aquifers, **V** and the reaction parameters in (5) are random space functions (RSFs); consequently, the solutions C and S are random. In applications, we may require the statistics of the tracer concentration, mass flux, or discharge.

Consider the case where the boundary conditions are given in (7); we may be interested in the expected value and variance of C, X, or J_1. The random character of C, X, S, etc., stems on the one hand from the random character of γ_X and γ_Y, and on the other hand from the possible randomness of the injection parameters, such as ΔM and q. A more comprehensive discussion on the effect of injection modes on nonreactive transport is given for instance in Ref. 24.

In this section, we focus on computing the expected values $\langle\gamma_X\rangle$ and $\langle\gamma_Y\rangle$. If ΔM is a deterministic parameter (this implies that ΔM is uniformly distributed over the injection area [see Fig. 1(a)]) then $\langle X\rangle = \Delta M\langle\gamma_X\rangle$ and $\langle Y\rangle = \Delta M\langle\gamma_Y\rangle$, i.e., the statistics of X and Y are equivalent to those of γ_X and γ_Y to a multiplicative constant.

The solutions of (8)–(10) are applicable for a single trajectory originating from **a**, and are dependent on **a**. If in reality the tracer is injected over a small area relative to the heterogeneity transverse integral scales (''non-ergodic'' transport[14]) the expected values will quantify ensemble statistics, i.e., uncertainty due to random heterogeneity. If the tracer release area is sufficiently large relative to the heterogeneity integral scale (''ergodic'' transport[14]) the expected values will represent field-scale values that in principle would be observed in single realizations of an aquifer by point-wise sampling of the concentration and mass flux over the ''control plane'' at x_1 [Fig. 1(a)], or the discharge by sampling over the entire CP. For the intermediate range (i.e., the transition from nonergodic to ergodic transport), a more comprehensive probabilistic analysis in the relative dispersion framework would be required (e.g., Ref. 25).

A. Reaction functions

The analytical solutions obtained for γ_X and γ_Y are random due to randomness of one, or several, of the Lagrangian quantities τ, ω, ν, ς, and μ. To provide a probabilistic solution of the problem, we require in the general case, the joint probability density function (PDF) for these quantities.

The expected value $\langle\gamma_X\rangle$, is computed from (23) as

$$\langle\gamma_X(t,x_1)\rangle = \int\int\int_0^t e^{-\varsigma-\omega} g(t-\mu,\mu,\omega,\varsigma;x_1)\,d\mu\,d\omega\,d\varsigma, \tag{26}$$

where $g(\tau,\mu,\omega,\varsigma)$ is a joint PDF at x_1; note that the integration over μ is limited to the interval $0,t$ to ensure $t-\mu>0$. For the equilibrium case, $\langle\gamma_X\rangle$ is obtained from (17) using the joint PDF $g(\tau,\mu;x_1)$:

$$\langle\gamma_X(t,x_1)\rangle = \int_0^t g(\tau,t-\tau;x_1)\,d\tau. \tag{27}$$

Equation (27) is a generalization of the equilibrium model for colloid-facilitated transport, applicable on the field scale for aquifers with spatially variable flow and sorption parameters.

The expected value, for instance, of γ_Y given in (24) can be computed similar to Eq. (26). However, for γ_Y we require a more complex joint PDF which also accounts for the spatial correlation of ν. The result is:

$$\langle\gamma_Y\rangle = \int_0^{x_1}\int\int\int\int\int_0^t e^{-\nu_x-\omega+\nu_\xi-\varsigma} \times \tilde{g}(t-\mu,\nu_x,\mu,\omega,\nu_\xi,\varsigma;x_1,\xi)\,d\mu\,d\omega\,d\nu_x\,d\nu_\xi\,d\varsigma\,d\xi, \tag{28}$$

where $\nu_x \equiv \nu(x_1)$ and $\nu_\xi \equiv \nu(\xi)$, and ς, ω, μ in the exponential are functions of ξ. The joint PDF $\tilde{g}$ is defined as

$$\tilde{g}(\tau',\nu',\mu'',\omega'',\nu'';x_1',x_1'') \equiv \int \alpha^* g(\alpha^*,\tau',\nu',\mu'',\omega'',\nu'';x_1',x_1'')d\alpha^*, \tag{29}$$

where $\alpha^* \equiv \alpha(x_1')/V_1(x_1')$, x_1' and x_1'' denote two separate locations along the mean flow direction x_1, and $\tau' \equiv \tau(x_1')$, $\mu'' \equiv \mu(x_1'')$, and equivalently for the other variables.

The joint PDF $\tilde{g}$ is a more complex form of the marginal PDF $\tilde{g}$ introduced in Ref. 11. Likewise, the random variables ν, μ, and ω are analogous to the random variable ''μ'' introduced in Ref. 12. Their joint statistics can be computed either using Monte Carlo simulations, or analytically based on small perturbation expansions (see results for τ,μ-statistics in Refs. 12, 26); further discussion on the computations of the PDFs in (26)–(28) are given in Appendix B.

In the special case where all mass transfer parameters are constant, and colloidal generation/removal is zero, i.e., $\epsilon=\chi=0$, we compute expected values as

$$\langle \gamma_X \rangle = \int \gamma_X(t,\tau) g(\tau;x_1) d\tau, \qquad \langle \gamma_Y \rangle = \int \gamma_Y(t,\tau) g(\tau;x_1) d\tau, \tag{30}$$

where $g(\tau;x_1)$ is the ground-water (nonreactive) tracer residence time distribution (or advective travel time PDF), from the injection plane at $x_1=0$, to the ''control plane'' at x_1, and γ_X and γ_Y are given in Appendix C.

In the general case, all the integrations in the above expressions have to be carried out numerically.

B. Temporal moments

An alternative approach to directly computing $\langle \gamma_X \rangle$ and $\langle \gamma_Y \rangle$, is to characterize $\langle \gamma_X \rangle$ and $\langle \gamma_Y \rangle$ by means of expected temporal moments.

Temporal moments m_p^X and m_p^Y ($p=0,1,2,\ldots$) are defined for a pulse of unit mass as

$$m_p^L(\tau) \equiv \int_0^\infty t^p \gamma_L(t,\tau) dt = (-1)^p \left. \frac{\partial^p \hat{\gamma}_L}{\partial s^p} \right|_{s=0}, \tag{31}$$

where $L=X,Y$; the generalization to continuous injection is straightforward.

The expected temporal moments are evaluated from (31) as

$$\langle m_p^L \rangle = (-1)^p \left. \frac{\partial^p \langle \hat{\gamma}_L \rangle}{\partial s^p} \right|_{s=0}. \tag{32}$$

Thus, we require $\langle \hat{\gamma}_X \rangle$ and $\langle \hat{\gamma}_Y \rangle$. The expected value, $\langle \hat{\gamma}_Y \rangle$, for instance, is computed from (19) as

$$\langle \hat{\gamma}_Y \rangle = \int_0^{x_1} \int\int\int\int\int\int e^{-\nu_x} \times \exp\{-s(\tau_x+\mu)+\nu_\xi-\omega-\varsigma\} \times \tilde{g}(\tau_x,\mu,\omega,\nu_x,\nu_\xi,\varsigma;x_1,\xi) \times d\tau d\omega d\mu d\nu_x d\nu_\xi d\varsigma d\xi, \tag{33}$$

where $\tau_x \equiv \tau(x_1)$, $\nu_x \equiv \nu(x_1)$, $\nu_\xi \equiv \nu(\xi)$, and $\tilde{g}$ is defined in an analogous manner as $\tilde{g}$ in (29); ς,ω,μ in the exponential are all functions of ξ.

In the case of uniform reaction parameters, the moments defined in (32) are random variables due to the randomness of τ only. We then compute

$$\langle m_p^L(x_1) \rangle = \int m_p^L(\tau) g(\tau;x_1) d\tau, \tag{34}$$

and the PDF of $m_p^L(\tau)$:

$$f(m_p^L) = \left| \frac{d\tau}{dm_p^L} \right| g[\tau(m_p^L);x_1], \tag{35}$$

where $\tau(m_p^L)$ is obtained by inverting $m_p^L(\tau)$; $\langle m_p^L \rangle$ in (34) is the first moment of the PDF $f(m_p^L)$. The use of temporal moments will be illustrated in the next section.

VI. APPLICATION EXAMPLES

For illustration purposes, we consider transport properties pertinent to the alluvial aquifer near Yucca Mountain, Nevada, where a site is being considered for a high-level nuclear waste repository (e.g., Ref. 27). The following hydraulic parameters have been estimated:[28] porosity $\vartheta=0.25$, geometic mean hydraulic conductivity $K_G=0.29$ km yr^{-1}, and the mean hydraulic gradient $\Omega_1=0.001\,73$ (set parallel to the x_1-direction). An isotropic integral scale of $\ln K$, and the variance of $\ln K$, were estimated as $I_{\ln K}=2$ km and $\sigma^2_{\ln K}=1.56$, respectively (see Appendix A for a brief description on ground-water flow with randomly varying K). The grain density of the aquifer material is 2500 kg m^{-3}, where from the bulk density is obtained as $\rho_b=(1-\vartheta)\times 2500=1875$ kg m^{-3}.

As a first-order estimate of the mean and variance of ground-water residence time, we use simple expressions (e.g., Ref. 29)

$$\langle \tau \rangle = \frac{L}{U} = 4\times 10^3 \text{ yr}, \qquad \mathrm{Var}(\tau) = \frac{2L\sigma^2_{\ln K} I_{\ln K}}{U^2} = 12.4\times 10^6 \text{ yr}^2, \tag{36}$$

where the transport distance for radionuclide transport in the alluvial aquifer is $L=8$ km. [The asymptotic expression for $\mathrm{Var}(\tau)$ (36) is obtained from (A2), Appendix A, for large $L/I_{\ln K}$; in our case $L/I_{\ln K}=4$. We argue in Appendix A that the asymptotic expression (36) for $\mathrm{Var}(\tau)$ will generally be

more accurate than the full expression (A2), in particular for $L/I_{\ln K}<5$.] The mean ground-water velocity is $U=K_G\Omega_1/\vartheta=0.002$ km yr^{-1}. With $\langle\tau\rangle$ and Var(τ) given in (36), the PDF $g(\tau;L)$ will be hypothesized as log-normal.[28]

We consider transport of two radionulcides: plutonium (Pu-239) and neptunium (Np-237). Neptunium is typically not considered as a tracer susceptible to colloid transport due to its relatively low sorption (compared, for instance, to plutonium). In fact, Penrose *et al.*[4] found very little neptunium associated with the particulate phase. However, Np is important in the performance assessment context,[30,31] due to its radiotoxicity,[32] long half-life, and low sorption. In addition, a large ''meta-data'' set on sorption parameters for Np in the Yucca Mountain alluvial aquifer is available in Ref. 33 and is suitable for sensitivity analysis.

From the available data set provided in Ref. 33, we estimated the geometric mean distribution coefficient for Np as 0.0144 m^3 kg^{-1}.[28] The dimensionless partitioning coefficient for Np is then $K_d=\rho_b\times 0.0144/\vartheta=108$, whereby the retardation coefficient is $R=109$. The half-life of Np is relatively large (2.14×10^6 yr), and we approximate the decay rate as zero. A data base for plutonium sorption properties in the alluvium aquifer, corresponding to the one for neptunium,[33] is not readily available. For comparative purposes, we shall use the plutonium sorption coefficient for granitic rocks of 5 m^3 kg^{-1} (Ref. 34, Table 12-1) (the neptunium sorption coefficient for granitic rocks suggested in Ref. 34, Table 12-1 is 0.01 m^3 kg^{-1} which turns out to be close to our average value of 0.0144 m^3 kg^{-1} for the alluvial aquifer) which yields a dimensionless sorption coefficient of $K_d=\rho_b\times 5/\vartheta=37\,500$. The half-life of Pu is about two orders-of-magnitude shorter than for Np (2.4×10^4 yr), and hence decay of Pu will be included in the computations.

Expected tracer discharge (or breakthrough) of neptunium at the ''control plane'' has been computed without accounting for colloid-facilitated transport.[28] An interesting application problem then is as follows: To what extent could colloids affect transport of Np, as well as of other radionuclides, such as Pu? In other words, to what extent could colloids enhance radionuclide discharge at the ''control plane?'' Parameters required for computing colloid-facilitated transport, such as C_c, ϵ, K_c, and α for the alluvial aquifer of the Yucca Mountain site are currently unavailable. We shall therefore illustrate a generic sensitivity of neptunium transport on the reversible rates α_f and α_r, and of neptunium and plutonium transport on the irreversible rate $\alpha=\alpha_f/R_c$. For simplicity, we consider only kinetic sorption sites on colloids, and set $\kappa\approx0$, whereby $R_c=1$.

A. Expected radionuclide discharge

For computations of the expected radionuclide discharge (or breakthrough) we shall consider the case of irreversible sorption on colloids for which the ''reaction functions'' γ_X and γ_Y are given in (C6). The expected values are computed from (C6) as

$$\langle\gamma_X\rangle=\frac{1}{R'}e^{-\alpha t/R'-\lambda t}g(t/R';x_1),$$

$$\langle\gamma_Y\rangle=\frac{\alpha}{K_d'}e^{-\alpha t/K_d'-\lambda t}\left[\int_0^t e^{\alpha\tau/K_d'}g(\tau;x_1)\,d\tau-\int_0^{t/R'}e^{\alpha\tau/K_d'}g(\tau;x_1)\,d\tau\right], \tag{37}$$

where $g(\tau;x_1)$ is the ground-water (or nonreactive tracer) residence time. Since $R_c=1$, $K_d'=K_d$ and $R'=R$. Equations (37) quantify expected tracer breakthrough at the ''control plane'' [Fig. 1(a)] at $x_1=L$, for unit injected radionuclide mass. (In this case reference to the ''accessible environment'' [Fig. 1(a)] is appropriate: After crossing the ''control plane,'' radionuclides would be ''accessible'' for humans and/or ecosystems, for instance, in a discharge/pumping area for drinking water, or a river. For risk assessment, expected radionuclide concentration can be computed from expected radionuclide discharge, based on the estimated rate of ground-water flow which mixes radionuclides as they are discharged into the ''accessible environment'' (e.g., Ref. 35). If we were solving a real case where the input is other than a pulse, the solutions (37) would need to be convoluted with the given injection rate.) Note that in (37), we have incorporated linear decay with the rate λ [T^{-1}].

With ground-water residence time moments (36) and a log-normal PDF $g(\tau;L)$, with $K_d=108$ for Np and $K_d=37\,500$ for Pu, we compute $\langle\gamma_Y\rangle$ using (37), for a six order-of-magnitude range of α values. The quadratures in (37) are carried out numerically. The results are illustrated in Fig. 2 and compared with $\langle\gamma_X\rangle$ when $\alpha=0$, which corresponds to the case of negligible effect of colloids.

Since colloids follow the ground-water, the first arrival of both Np and Pu essentially coincides with that of the ground-water (or a nonreactive tracer). The precise time of first arrival for colloid-bounded radionuclide is weakly dependent on the value of the rate α (Fig. 2). The magnitude of the expected radionuclide discharge, and in particular the peak, is strongly dependent on α: the six order-of-magnitude range for α yields a six–seven order-of-magnitude range for the peak values both for Pu and Np (Fig. 2).

Comparison between $\langle\gamma_Y\rangle$ and $\langle\gamma_X\rangle$ indicates that the difference in the peaks is much larger for Pu than Np, because Pu is subject to strong sorption on the porous matrix, as well as to decay. If the impact of colloids is neglected, the first arrival of Pu is after 3×10^4 years with a relatively low peak; the breakthrough terminates after about 10^6 years. The peak of the colloid-bounded Pu discharge can be considerably larger than that for the dissolved Pu, depending on α, and is attained already after approximately 1000 years [Fig. 2(b)]. For the highest irreversible sorption rate considered ($\alpha=10^{-3}$ yr^{-1}), the effect of colloid-facilitated transport is dramatic: the peak for colloid-bounded Pu exceeds $\langle\gamma_X\rangle$ by 15 orders-of-magnitude [Fig. 2(b)]. We emphasize that the curves in Fig. 2 are applicable only if the removal/generation of colloids is negligible; these curves could be affected sig-

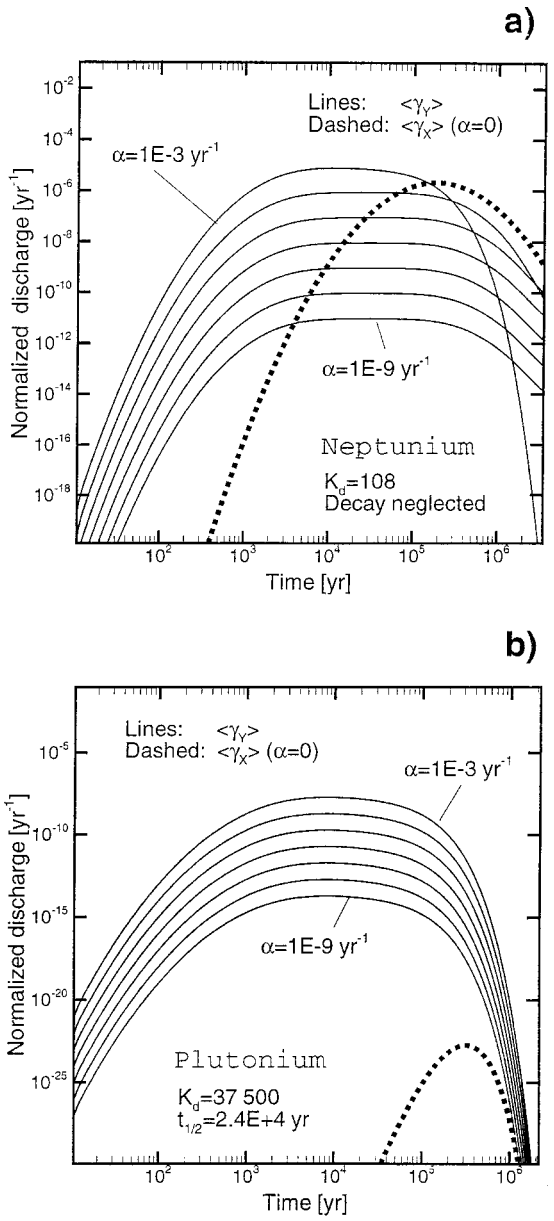

FIG. 2. Sensitivity of the expected normalized discharge [Eq. (37)] to the irreversible mass transfer rate α for (a) neptunium, (b) plutonium. The ground-water residence time parameters $\langle\tau\rangle=4\times10^3$ yr and $\sigma_\tau^2=12.4\times10^6$ yr^2 are those estimated for the Yucca Mountain site, Nevada (Ref. 28); $g(\tau)$ is assumed log-normal. K_d for neptunium is from Ref. 33, and K_d for plutonium is from Ref. 34.

nificantly if colloidal removal/generation is accounted for, depending on the rates ϵ and χ (see Sec. IV B).

The impact of the two controlling sorption parameters in (37) K_d and α, is apparent in Fig. 2. A pulse of a strongly sorbing tracer (such as Pu) moves slowly through the aquifer and in a sense acts as a continuous source for the colloid-bounded tracer; hence the colloid-bounded tracer breakthrough is greatly extended over time. Stronger sorption also implies lower magnitudes of the colloid-bounded tracer discharge, since more tracer mass in attached to the porous matrix and less tracer mass is available for irreversible sorption on colloids; hence the maximum discharge is lower for Pu than for Np, approximately three orders-of-magnitude [Figs. 2(a) and 2(b)], due to both larger K_d for Pu and decay of Pu.

It is peculiar that even an irreversible sorption rate as low as $\alpha=10^{-9}$ yr^{-1} yields an effect which may be observable at the ''control plane.'' If we define an ''intrinsic'' irreversible rate as $\alpha_0=\alpha/C_c$ (a rate per unit colloidal concentration, see Secs. III D and IV B), then with a typical value of say $C_c=10^{-3}$ kg m^{-3}, $\alpha=10^{-9}$ yr^{-1} yields $\alpha_0=10^{-6}$ yr^{-1} m^3 kg$^{-3}=3.17\times10^{-17}$ s^{-1} l mg^{-3}. For $\alpha=10^{-3}$ yr^{-1}, the corresponding intrinsic rate would be $\alpha_0=3.17\times10^{-11}$ s^{-1} l mg^{-3}. These values may be difficult to determine under laboratory conditions. For instance, ''intrinsic'' rates obtained for reversible sorption of cesium on kaolinite particles in laboratory columns are of the order $10^{-6}-10^{-7}$ s^{-1} l mg^{-3} (Ref. 7) (the range of colloidal concentrations C_c used in the experiments of Ref. 7 was 0.05–0.2 kg m^{-3}).

Since the decay of Np is relatively low, and Np sorbs on the porous matrix weakly compared to Pu, the overall effect of colloids of Np is modest compared to Pu. The maximum peak of the colloid-bounded Np discharge (for $\alpha=10^{-3}$ yr^{-1}) is approximately the same as that of the dissolved Np when colloids are not present, whereas the first arrival is reduced by approximately one order-of-magnitude [Fig. 2(a)].

B. Relative CFTT-indicators

In the following, we shall use temporal moments (31), to define relative (dimensionless) indicators for colloid-facilitated tracer transport (CFTT):

$$\begin{aligned}
\mu_X &\equiv \langle m_0^X\rangle = \int m_0^X g(\tau;x_1)\,d\tau,\\
\mu_Y &\equiv \langle m_0^Y\rangle = \int m_0^Y g(\tau;x_1)\,d\tau,\\
\theta_X &\equiv \frac{1}{\langle\tau\rangle R}\int\left(\frac{m_1^X}{m_0^X}\right) g(\tau;x_1)\,d\tau,\\
\theta_Y &\equiv \frac{1}{\langle\tau\rangle R}\int\left(\frac{m_1^Y}{m_0^Y}\right) g(\tau;x_1)\,d\tau.
\end{aligned} \tag{38}$$

θ's and μ's defined in (38) provide *in pairs*, relevant information on the degree to which colloids may be expected to enhance contaminant transport; they can be useful for screening purposes in environmental assessment. We shall illustrate CFTT-indicators (38) for Np, with $R\equiv1+K_d=109$, for *reversible* sorption on colloids with α_f and α_r as the controlling parameters. Given the ground-water residence time moments (36) and a log-normal $g(\tau;L)$, we shall highlight in a generic manner the effect of rates α_f and α_r on Np transport.

In the absence of colloids (i.e., for $\alpha_f=\alpha_r=0$), $\mu_X=1$ and $\theta_X=1$, whereas $\mu_Y=0$ and θ_Y is not defined. Thus values of μ_X and θ_X close to unity imply that the effect of colloids on tracer transport is small. If the effect of colloids is sufficiently strong and tracer transport is by colloids only, then $\mu_X=0$ and θ_X is not defined, whereas $\mu_Y=1/(1+K_d)$ and $\theta_Y=1$; in other words, tracer mobility is significantly

enhanced and the entire tracer mass arrives with ground-water, $1+K_d$ times faster compared to the case where colloids are not present.

Small θ_Y indicates rapid transport, however, if the rapidly transported tracer mass is small, then the effect is still negligible. The relative amount of tracer mass arriving at the ''control plane'' on colloids is quantified by μ_Y. From the environmental assessment point of view, the unfavorable combination is small θ_Y with sufficiently large (nonnegligible) μ_Y, which implies a significant enhancement of tracer transport by colloids. The degree to which colloids enhance transport depends on the rates α_f and α_r, the special case being irreversible sorption ($\alpha_r=0$).

The indicators (38) are computed by numerical quadratures using the ''reaction functions'' defined in (C9), and are plotted in the log-parameter space $[\log D_m, \log(\alpha_f/\alpha_r)]$ in Figs. 3 and 4. $D_m \equiv \langle \tau \rangle \alpha_r$ is the Damkohler number. For large D_m, colloid-tracer exchange is under equilibrium. The equilibrium range is clearly indicated in Figs. 3 and 4 by the vertical isolines, where already for $D_m > 10$, θ's and μ's are independent of D_m. In the limit $D_m \to 0$ (which also implies $\alpha_f \to 0$, since the ratio α_f/α_r is finite), colloids do not affect transport.

The patterns for θ_X and θ_Y are different, with a relatively large region where the value of θ_Y is around 0.5 [Figs. 3(a) and 4(a)]. In comparison, μ_X and μ_Y have identical patterns with complementary values [Figs. 3(b) and 4(b)]. The isoline patterns of θ_X, μ_X are similar, with essentially overlapping values, implying that a significant mass fraction transported in solution (i.e., large μ_X) is always associated with large (retarded) residence time (i.e., large θ_X), and vice versa, due to the retardation of the dissolved tracer. By contrast, θ_Y, μ_Y have dissimilar patterns and nonoverlapping values. In other words, in a substantial region of the parameter space, low θ_Y can be associated with relatively high μ_Y, indicating rapid transport of nonnegligible tracer mass. It is of particular significance to accurately estimate D_m in this region. Neglecting kinetic effects for $D_m < 10$ may result in considerable underestimation of the colloidal impact on tracer migration. If simultaneously $D_m \to 0$ and $\alpha_f/\alpha_r \to \infty$, we obtain the irreversible limit, summarized by (18).

Finally, we note the relationship between the expected discharge curves of Fig. 2(a) and dimensionless indicators of Fig. 4. The area under the curves $\langle \gamma_Y \rangle$ in Fig. 2(a) is μ_Y of Fig. 4, i.e., $\mu_Y = \int \langle \gamma_Y \rangle \, dt$, whereas the mean residence time for Np is $\int t \langle \gamma_Y \rangle dt = \langle m_1^Y \rangle$ which is approximately $\mu_Y \theta_Y$ (since $\theta_Y = \langle m_1^Y / m_0^Y \rangle$). In Fig. 2 we consider the irreversible sorption limit, whereas in Fig. 4 we consider reversible sorption. Thus the region in the parameter space of Fig. 4 where α_f is large compared to α_r roughly corresponds to the irreversible case of Fig. 2.

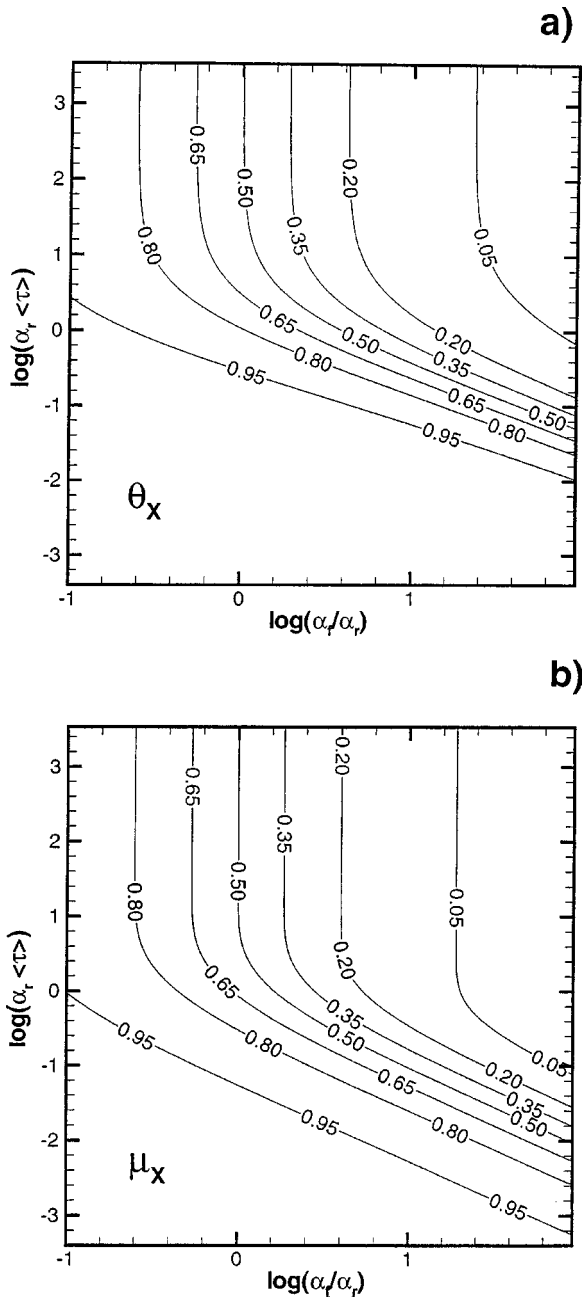

FIG. 3. Dimensionless parameters [Eq. (38)] for dissolved neptunium as a function of dimensionless tracer-colloid (reversible) exchange rates, α_f and α_r: (a) θ_X and (b) μ_X. The ground-water residence time parameters $\langle \tau \rangle = 4 \times 10^3$ yr and $\sigma_\tau^2 = 12.4 \times 10^6$ yr^2 are those estimated for the Yucca Mountain site, Nevada (Ref. 28); $g(\tau)$ is assumed log-normal. K_d for neptunium is from Ref. 33.

VII. CONCLUSIONS

We derived solutions for γ_X and γ_Y that quantify reactive solute transport in a three-phase system (fluid-porous matrix-colloids), and can be used for computing dissolved and/or colloid-bounded tracer concentration, discharge, or mass flux in aquifers. The derived solutions are applicable for equilibrium and irreversible sorption of the tracer onto colloids, where reaction parameters, including colloidal concentration, are spatially variable or uniform (Appendix C). The results in this work were obtained based on three key assumptions: (i) the physical transport is advection-dominated, i.e., effects of pore-scale dispersion are negligible; (ii) colloidal concentration varies in space but not in time; (iii) all mass transfer reactions are linear.

The statistical computations of the reaction functions γ_X and γ_Y, involve, in the general case, joint statistics of Lagrangian quantities ν, ς, μ, ω, and τ, which depend on the

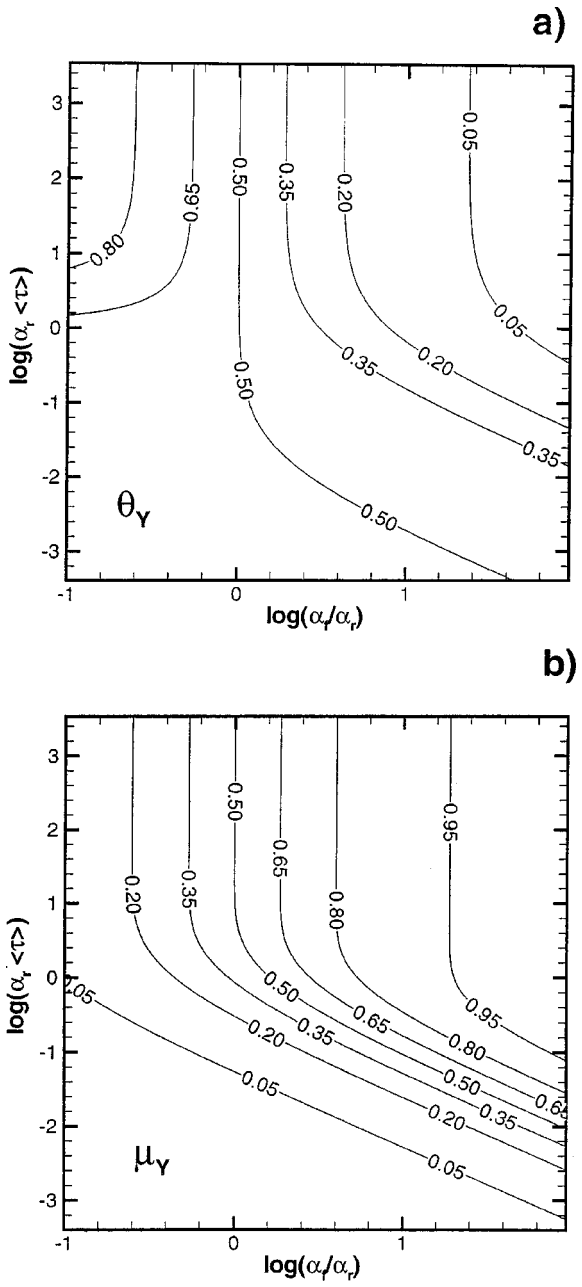

FIG. 4. Dimensionless parameters [Eq. (38)] for colloid-bounded neptunium as a function of dimensionless tracer-colloid (reversible) exchange rates, α_f and α_r: (a) θ_Y and (b) μ_Y. The ground-water residence time parameters $\langle\tau\rangle = 4\times10^3$ yr and $\sigma_\tau^2 = 12.4\times10^6$ yr^2 are those estimated for the Yucca Mountain site, Nevada (Ref. 28); $g(\tau)$ is assumed log-normal. K_d for neptunium is from Ref. 33.

Eulerian statistics of the hydraulic conductivity and reaction parameters. The moments of ν, ς, μ, ω, and τ can be determined analytically based on first-order expansions, or numerically using Monte Carlo simulations; the methodology would be analogous to the one applied in Ref. 12 (see also Ref. 26) for a simpler problem of transport in aquifers with spatially variable sorption properties. A discussion on the computation of the joint statistical moments of ν, ς, μ, ω, and τ, is given in Appendix B.

The present results enable sensitivity analysis of varying complexity, from homogeneous conditions and constant C_c, to randomly varying reaction parameters (including the steady-state colloidal concentration, C_c), reversible and irreversible exchanges, equilibrium and nonequilibrium exchange, on one or two sites. Such analysis would aid in setting constraints on future laboratory and field investigations designed to more accurately assess the significance of colloid-facilitated tracer transport in aquifers.

The applicability of the general result (28) was illustrated for the special case of spatially uniform reaction parameters, where colloid removal and generation are neglected. In particular, we used (37) for computing expected discharge of plutonium and neptunium in the alluvial aquifer of the Yucca Mountain site, Nevada. A generic sensitivity analysis indicates that the effect of colloids may be dramatic, depending on the irreversible transfer rate α, in particular for plutonium. Even an extremely low irreversible rate α (which may be difficult to measure in the laboratory), can apparently yield observable effects.

Suitable dimensionless indicators (38) were proposed for assessing the potential impact of colloid-facilitated tracer transport (CFTT) in aquifers. Using the PDF $g(\tau)$ pertinent to the alluvial aquifer near Yucca Mountain, Nevada, CFTT-indicators (38) were shown to be sensitive to the reversible kinetic rates of the tracer-colloid interaction, α_f, α_r. Of particular interest is the range of kinetic rates far from equilibrium for which essentially irreversible mass transfer takes place. Plotted sensitivity curves indicate that accurate estimates of kinetic rates α_f and α_r under field conditions, may indeed be important when assessing the extent to which tracer transport in ground-water is affected by colloids; a similar conclusion has been drawn for laboratory conditions (e.g., Refs. 7, 8). The curves in Figs. 3 and 4 may be used for a site-specific assessment of the colloidal impact, provided that the parameters K_c, α_f, and α_r can be estimated based on available field and laboratory data.

Several extensions of the present results are possible. Reaction functions of Appendix C can be incorporated into the semianalytical framework of Ref. 36 for analyzing colloid-facilitated contaminant transport in a soil-groundwater system, which is of particular interest for organic pollutants. Likewise, the reaction functions in Appendix C can be directly incorporated into the relative dispersion framework of Ref. 25, which is useful in analyzing the fate of relatively small contaminant plumes in a risk assessment context.

For risk assessment of subsurface contaminants, it is of interest to compute higher-order moments (e.g., variance) of the tracer discharge, or the mass flux, where pore-scale dispersion plays an important role. (This role is analogous to the one molecular diffusion plays in turbulent diffusion.) A methodology is available for computing the concentration variance within the Lagrangian framework, where the effect of pore-scale dispersion is accounted for.[37] The methodology of Ref. 37 has been recently extended for computing the variance of the mass flux for reactive solute.[38] The quantities required for extending the methodology of Ref. 38 and computing the variance of mass flux (or discharge) for dissolved as well as colloid-bounded tracer, are the derived reaction functions [Eqs. (15)–(17), (21)–(24)].

ACKNOWLEDGMENTS

The author wishes to thank several colleagues for reading an early version of the manuscript and providing constructive comments: D. Turner and S. Painter, CNWRA, Southwest Research Institute, St. Antonio, Texas; G. Dagan, Tel-Aviv University, Israel; P. Martinet and S. Berglund, Royal Institute of Technology, Stockholm, Sweden. This manuscript was prepared to document work performed for the Center for Nuclear Waste Regulatory Analysis (CNWRA) on behalf of the U.S. Nuclear Regulatory Commission (NRC). The manuscript is an independent product and does not necessarily reflect the views or regulatory position of the NRC.

APPENDIX A: GROUND-WATER FLOW AND ADVECTIVE TRANSPORT

We consider ground-water flow in an aquifer with spatially variable hydraulic conductivity, $K(\mathbf{x})$, where $\mathbf{x}(x_1,x_2,x_3)$ is a Cartesian coordinate vector. The spatial variability of the hydraulic conductivity encountered in aquifers is set into a rational framework by regarding $K(\mathbf{x})$ as a random space function (RSF).

The ground-water velocity $\mathbf{V}(V_1,V_2,V_3)$ satisfies the continuity equation $\nabla\cdot(\vartheta\mathbf{V})=0$, and is related to K, the porosity ϑ, and to the hydraulic head Φ through Darcy's law $\mathbf{V}=-(K/\vartheta)\nabla\Phi$; consequently, $\mathbf{V}$ is a RSF. The support scale for $\mathbf{V}$ is what is referred to as the local (or laboratory) scale [Fig. 1(b)].

The common assumption is that K is log-normally distributed,[15] i.e., $\ln(K/K_G)$ is $N(0,\sigma^2_{\ln K})$ where K_G is the geometric mean of K. An (an)isotropic negative exponential covariance is usually employed in geostatistical models of the hydraulic conductivity, where the integral scales of $\ln K$ are inferred from field data.[15] In the isotropic case, one integral scale is required, $I_{\ln K}$.

Ground-water flow through aquifers is generally steady or changes slowly, hence we assume steady-state conditions. The flow is driven by field-scale, steady boundary conditions that impose an average constant hydraulic gradient, $\mathbf{\Omega}$. Because the variations in porosity are relatively small, a common assumption is that of uniform porosity. The statistics of $\mathbf{V}$ have been related to the statistics of K both analytically using first-order approximations (e.g., Ref. 39), and numerically using Monte Carlo simulations (e.g., Ref. 40).

A nonreactive and dynamically inert tracer injected at $\mathbf{x}=\mathbf{a}(0,a_2,a_3)$ [Fig. 1(b)] is advected as an indivisible entity, referred to as a tracer parcel. The support scale for the tracer parcel is the local scale [Fig. 1(b)]; thus the tracer parcel consists of many tracer and colloidal particles. The parcel advection trajectory is $\mathbf{X}(t;\mathbf{a})$ $[X_1(t;\mathbf{a}),X_2(t;\mathbf{a}),X_3(t;\mathbf{a})]$, with $\mathbf{X}(0;\mathbf{a})=\mathbf{a}$, where $\mathbf{X}$ is obtained by solving $d\mathbf{X}(t;\mathbf{a})/dt=\mathbf{V}[\mathbf{X}(t;\mathbf{a})]$.[41,14]

A useful parametrization of Lagrangian variables is in terms of x_1, i.e., the position parallel to the mean flow (e.g., Refs. 10, 13). The solution of $x_1-X_1(t;\mathbf{a})=0$ yields $t=\tau(x_1;\mathbf{a})$ where $\tau=0$ for $x_1=0$. Hence τ is the advective travel time from $x_1=0$ to x_1. Note that if $x_1-X_1(t;\mathbf{a})=0$ has multiple roots, we select the first passage time. Next we define $\eta(x_1;\mathbf{a})=X_2(\tau;\mathbf{a})$ and $\zeta(x_1;\mathbf{a})=X_3(\tau;\mathbf{a})$ where $x_2=\eta$ and $x_3=\zeta$ pertain to the trajectory. The Lagrangian quantities τ and η,ζ satisfy differential equations $d\tau/dx_1=1/V_1(x_1,\eta,\zeta)$ $d\eta/dx_1=V_2(x_1,\eta,\zeta)/V_1(x_1,\eta,\zeta)$ and $d\zeta/dx_1=V_3(x_1,\eta,\zeta)/V_1(x_1,\eta,\zeta)$ with $\eta(0;\mathbf{a})=a_2$ and $\zeta(0;\mathbf{a})=a_3$.

Ground-water (or nonreactive tracer) residence time, τ, is defined in an integral form as

$$\tau(x_1;\mathbf{a})=\int_0^{x_1}\frac{dx}{V_1[x,\eta(x;\mathbf{a}),\zeta(x;\mathbf{a})]}, \tag{A1}$$

which has served as a basis for analytical (approximate) or numerical computations of τ statistical moments (e.g., Refs. 12, 29). For instance, the first-order expression for $\mathrm{Var}(\tau)$ in a three-dimensional, statistically isotropic, heterogeneous aquifer is

$$\frac{\mathrm{Var}(\tau)U^2}{I_{\ln K}\sigma^2_{\ln K}}=2\left[\xi-\frac{8}{3}+\frac{4}{\xi}-\frac{8}{\xi^3}+\frac{8}{\xi^2}\left(1+\frac{1}{\xi}\right)e^{-\xi}\right], \tag{A2}$$

where $\xi=x_1/I_{\ln K}$. Note that at first-order, (A2) is identical in form to the longitudinal displacement variance derived first in Ref. 14, Eq. (4.9). For $\xi\to\infty$, we obtain the asymptotic expression for $\mathrm{Var}(\tau)$ (36). Clearly (36) for $\mathrm{Var}(\tau)$ overestimates the pre-asymptotic value (A2), in particular for relatively small $x_1/I_{\ln K}$. However, three-dimensional numerical simulations have shown that (A2) underestimates simulated values for $\sigma^2_{\ln K}=1$ (Ref. 24, Fig. 2). Hence applying (36) rather than (A2) for $\mathrm{Var}(\tau)$ at $L/I_{\ln K}=4$ is likely to be more accurate [see Fig. 2(c) in Ref. 24].

Any Eulerian quantity $Q(\mathbf{x})$ can be transformed to obtain its Lagrangian counterpart, either as a function of τ, or x_1. In particular,

$$Q(\tau)=Q[\mathbf{X}(\tau)],\quad Q(x_1)=Q[x_1,\eta(x_1),\zeta(x_1)].$$

Note that $Q(\mathbf{x}),Q(\tau)$, and $Q(x_1)$ are all different functions, however, the same notation is retained for simplicity. Furthermore, a gradient $\nabla\cdot(Q\mathbf{V})$ where $Q(t,\mathbf{x})$, is transformed onto a trajectory (stream tube) as $dQ/d\tau$, where $Q(t,\tau)$.[10] Using $d\tau=dx_1/V_1$, we also have

$$\int_0^{\tau}Q(\theta)d\theta=\int_0^{x_1}\frac{Q(\xi)}{V_1}d\xi.$$

APPENDIX B: LAGRANGIAN STATISTICS

Computation of expected values in Secs. V A–V B require (joint) probability density functions (PDFs), of one or several Lagrangian variables: τ, μ, ν, ω, and ς. The basis for determining these PDFs are, on the one hand, the Eulerian fields of the reaction parameters (α, ϵ, χ, $\mathcal{P}$) with given statistics, and on the other hand, the statistics of the hydraulic conductivity, K, as well as the boundary conditions (e.g., a mean hydraulic gradient), for solving ground-water flow (see Appendix A).

The Lagrangian PDFs of Secs. V A–V B can be computed from the Eulerian statistics only approximately. The two principal approaches are *analytical* using the small perturbation approximation, and *numerical* using Monte Carlo

simulations. The analytical approach assumes that the trajectories are approximately parallel to the mean flow, whereby the Eulerian and Lagrangian statistics are related in a simple manner.[15]

The simplest PDF considered here is for the groundwater residence time, τ, $g(\tau)$, used in (30), (34), and (37)–(38), where all reaction parameters are assumed spatially uniform. The PDF $g(\tau)$ has been the subject of several investigations, analytical and numerical. One analytical approach is to derive the first two moments of τ based on small perturbation approximation, and then assume a particular form of $g(\tau)$; a common form is the log-normal distribution. Alternatively, $g(\tau)$ can be expressed as a function of the PDF of the trajectory $\mathbf{X}$, $g(\mathbf{X})$.[15] Both approaches are approximate, since only the first two moments are computed analytically (of τ or $\mathbf{X}$), and the actual form of the PDFs [$g(\tau)$ or $g(\mathbf{X})$] has to be hypothesized. Both analytical approaches yield comparable results and have been verified by numerical simulations.[40,11] For large variability in K, the approximate analytical results are not applicable, and the determination of $g(\tau)$ has to rely on numerical Monte Carlo simulations (e.g., Refs. 40, 11).

Joint PDFs for Lagrangian random variables which integrate reaction parameters along a trajectory $\mathbf{X}$, are used in (26)–(27). The moments of these PDFs can be computed analytically using first-order expansions as presented in Ref. 12. The approach in Ref. 12 was to compute the first two moments of the two random variables τ and μ (including the joint moment) and then assume a particular (log-normal) joint PDF. In Ref. 12, we compared the analytical (approximate) results with results from two-dimensional numerical simulations, and found a reasonable agreement for small to moderate variability in the hydraulic conductivity and reaction parameter. The approach of Ref. 12 can be extended to several random variables, relevant for the joint PDF in (26).

The most complex PDFs considered here are given in (28), (29), and (33). These involve different Lagrangian variables at two different locations. In principle, the same analytical methodology can be applied as that used in Ref. 12, however, the computations would be more comprehensive, since more complex correlations are involved. Monte Carlo simulations would essentially be the same as those in Ref. 12 for two-dimensional aquifers and in Ref. 26 for three-dimensional aquifers, except that more variables need to be considered.

Specifically, simulations of advective (nonreactive) transport are required for computing the joint PDF, for instance, in (29). The first step is generating on a grid realizations of the K field and solving subsequently the flow equations to obtain the velocity $\mathbf{V}$ and the associated Lagrangian variables $\tau(x_1;\mathbf{a}), \eta(x_1;\mathbf{a})$, and $\zeta(x_1;\mathbf{a})$, which depict the trajectories of the fluid flow and advective transport. In parallel, fields of $\epsilon(x_1,\eta,\zeta)$, $\alpha(x_1,\eta,\zeta)$, $\chi(x_1,\eta,\zeta)$, and $\mathcal{P}(x_1,\eta,\zeta)$ are generated on the same grid by using the given Eulerian statistics. Once this step is accomplished, random variables ν, μ, and ω are derived by quadratures along the trajectory. In addition to the random variables which integrate reaction parameters, we also consider the ratio α/V_1 and ς along the trajectory. It is emphasized that for the steady flows considered here, the time variable is not involved in the computation steps, and only the spatial distributions of the aforementioned variables is required. The main practical task with the simulations would be to test various correlations and provide a basis for simplified analytical models of the joint PDFs.

APPENDIX C: UNIFORM CASE

The coupled Lagrangian system (8) accounts for spatial variability in the ground-water velocity through τ. If reaction parameters in (8) are random space functions, then we require field data on their statistics (e.g., mean, auto-, and cross-covariances, etc.). In many applications, however, only a few samples may be available for determining the sorption properties, insufficient for a statistical description. In these cases, the available data would be used to provide the best estimate of effective (uniform) parameter values.

Here we assume that $\epsilon=\chi=0$, i.e., $C_c=C_c^0$ is uniform in the domain of interest, and that the reaction parameters in (8) are spatially uniform. We consider ''nonideal'' transport ($\psi_{\rm pm}\neq 0$), and give examples for the common reversible linear sorption–desorption model (e.g., Refs. 16, 10),

$$\psi_{\rm pm}\equiv -k_f\gamma_X+k_rN_X, \quad \mathcal{F}\equiv\frac{sk_f'}{s+k_r'},$$
$$k_f'\equiv k_f/R_c, \quad k_r'\equiv k_r/R_c, \tag{C1}$$

where k_f is the forward, and k_r the reverse rate. We see in (C1) that the kinetic sorption rates for the porous matrix are reduced by a factor R_c, due to the presence of colloids,

The boundary conditions for γ_X and γ_Y are $\gamma_X(t,0)=\delta(t)$ and $\gamma_Y(t,0)=0$ with an initially tracer-free porous medium, $\gamma_X(0,\tau)=\gamma_Y(0,\tau)=0$.

Irreversible sorption

With $\alpha_r=0$ and $\alpha\equiv\alpha_f/R_c^0$, we get from (8)–(10) with $\nu=0$, $\omega=\alpha\tau$, $\mu=K_d\tau/R_c^0$,

$$\hat{\gamma}_X=\exp[-(s+A)\,\tau],$$
$$\hat{\gamma}_Y=\frac{\alpha}{A}\exp(-s\tau)\{1-\exp[-A\,\tau]\}, \tag{C2}$$

where

$$A\equiv sK_d'+\alpha+\mathcal{F},$$
$$K_d'\equiv\frac{K_d}{R_c^0}, \quad R_c^0=1+\kappa C_c^0, \tag{C3}$$

and $\mathcal{F}$ is arbitrary. With $\mathcal{F}$ defined in (C1) (where $R_c\equiv R_c^0$), inversion of (C2) with (C3) yields

$$\gamma_X(t,\tau)=\exp(-\alpha\tau)\,\gamma(t-K_d'\tau,\tau), \tag{C4}$$

$$\gamma_Y(t,\tau)=\alpha\int_0^t f(t-t')h(t',\tau)dt', \tag{C5}$$

where

$$h(t,\tau)\equiv\delta(t-\tau)-\exp(-\alpha\tau)\,\gamma(t-K_d'\tau,\tau),$$

$$f(t)\equiv e^{pt}\left[\cosh(qt)+\frac{k_r'+p}{q}\sinh(qt)\right],$$

$$p\equiv-\frac{1}{2K_d'}(K_d'k_r'+\alpha+k_f'),\quad q^2\equiv p^2-\frac{\alpha k_r'}{K_d'},$$

and

$$\begin{aligned}\gamma(t,\tau)&\equiv\mathcal{L}^{-1}\{\exp[-\tau(s+\mathcal{F})]\}\\&=e^{-\tau k_f'}\delta(t-\tau)\\&\quad+\tau k_f'k_r'\exp\{-[k_f'\tau+k_r'(t-\tau)]\}\\&\quad\times\tilde{I}_1[k_f'k_r'\tau(t-\tau)]H(t-\tau)\end{aligned}$$

is the reaction function for linear reversible sorption–desorption, with $\tilde{I}_1(Z)\equiv I_1(2Z^{1/2})/Z^{1/2}$, and I_1 being the modified Bessel function of the first kind of order one (e.g., Ref. 10).

The case of equilibrium sorption on the porous matrix is formally obtained by setting $\mathcal{F}=0$. Equivalently, the equilibrium case is obtained in the limit as kinetic rates become large; then $\mathcal{F}\sim s$, say $\mathcal{F}=B\,s$, and B can be incorporated into K_d. γ_X and γ_Y are for the equilibrium case given by (23)–(24) which here reduce to

$$\begin{aligned}\gamma_X(t,\tau)&=\exp(-\alpha\tau)\,\delta[t-(1+K_d')\tau],\\\gamma_Y(t,\tau)&=\frac{\alpha}{K_d'}\exp\left[-\frac{\alpha(t-\tau)}{K_d'}\right][H(t-\tau)\\&\quad-H(t-\tau-K_d'\tau)].\end{aligned}\tag{C6}$$

In the case where $K_d'=0$ and $R'=1$, i.e., tracer sorption onto the porous matrix is negligible, we get simple expressions

$$\gamma_X(t,\tau)=e^{-\alpha\tau}\delta(t-\tau),\quad\gamma_Y(t,\tau)=(1-e^{-\alpha\tau})\,\delta(t-\tau),$$

where the pure advective case is obtained for total tracer discharge (in water and on colloids) as $\gamma_X+\gamma_Y=\delta(t-\tau)$.

Reversible sorption

With $\epsilon=\chi=0$ and constant reaction parameters, Laplace transform of (8)–(11), yields

$$\begin{aligned}\frac{d\hat{\gamma}_X}{d\tau}&=a_{11}\hat{\gamma}_X+a_{12}\hat{\gamma}_Y,\\\frac{d\hat{\gamma}_Y}{d\tau}&=a_{21}\hat{\gamma}_X+a_{22}\hat{\gamma}_Y,\end{aligned}\tag{C7}$$

where the components of a_{ij} are defined by

$$\begin{aligned}a_{11}&=-[s(1+K_d')+\alpha_f+\mathcal{F}],\\a_{12}&=\alpha_r,\quad a_{21}=\alpha_f,\quad a_{22}=-(s'+\alpha_r).\end{aligned}\tag{C8}$$

Note that both α_f and α_r are scaled by R_c^0. In other words, the rates which would be estimated (if possible) in the absence of equilibrium sorption need to be reduced by a factor $R_c>1$, if parallel equilibrium sorption on colloids takes place.

The solution of (C7) is

$$\begin{aligned}\hat{\gamma}_X(s,\tau)&=A_1\exp(\Lambda_1\tau)+A_2\exp(\Lambda_2\tau),\\\hat{\gamma}_Y(s,\tau)&=B_1\exp(\Lambda_1\tau)+B_2\exp(\Lambda_2\tau),\end{aligned}\tag{C9}$$

where

$$A_1=\frac{a_{11}-\Lambda_2}{\Lambda_1-\Lambda_2},\quad A_2=\frac{\Lambda_1-a_{11}}{\Lambda_1-\Lambda_2},$$

$$B_1=A_1\frac{\Lambda_1-a_{11}}{a_{12}},\quad B_2=-B_1,$$

$$\Lambda_{1,2}=\tfrac{1}{2}(a_{11}+a_{22})\pm\tfrac{1}{2}[(a_{11}-a_{22})^2+4a_{12}a_{21}]^{1/2}.$$

Once $\hat{\gamma}_X$ and $\hat{\gamma}_Y$ are computed from (C9), γ_X and γ_Y can be obtained by numerical inversion for any $\mathcal{F}$. An analytical approach is to characterize γ_X and γ_Y by temporal moments (31)–(32), where $\hat{\gamma}_X$ and $\hat{\gamma}_Y$ are given in (C9); this approach has been used for illustration in Sec. VI B.

[1] J. F. McCarthy and J. M. Zachara, ''Subsurface transport of contaminants,'' Environ. Sci. Techn. **23**, 496 (1989).
[2] A. B. Kersting, D. W. Efured, D. L. Finnegan, D. J. Rokop, D. K. Smith, and J. J. Thompson, ''Migration of plutonium in ground water at the Nevada Test Site,'' Nature (London) **397**, 56 (1999).
[3] B. D. Honeyman, ''Colloidal culprits in contamination,'' Nature (London) **397**, 23 (1999).
[4] W. R. Penrose, W. L. Polzer, E. H. Essington, D. M. Nelson, and K. A. Orlandini, ''Mobility of Plutonium and Americium through a shallow aquifer in a semiarid region,'' Environ. Sci. Technol. **24**, 228 (1990).
[5] R. C. Marty, D. Bennett, and P. Thullen, ''Mechanism of plutonium transport in a shallow aquifer in Mortandad Canyon, Los Alamos National Laboratory, New Mexico,'' Environ. Sci. Technol. **31**, 2020 (1997).
[6] M. Y. Corapcioglu and S. Jiang, ''Colloid-facilitated groundwater contaminant transport,'' Water Resour. Res. **29**, 2215 (1993).
[7] J. E. Saiers and G. M. Hornberger, ''The role of colloidal kaolinite in the transport of cesium through laboratory sand columns,'' Water Resour. Res. **32**, 33 (1996).
[8] L. Lührmann and U. Noseck, ''Model of contaminant transport in porous media in the presence of colloids applied to actinide migration in column experiments,'' Water Resour. Res. **34**, 421 (1998).
[9] Y. Ouyang, D. Shinde, R. S. Mansell, and W. Harris, ''Colloid-enhanced transport of chemicals in subsurface environments: A review,'' Crit. Rev. Environ. Sci. Technol. **26**, 189 (1996).
[10] V. Cvetkovic and G. Dagan, ''Transport of kinetically sorbing solute by steady random velocity in heterogeneous porous formations,'' J. Fluid Mech. **265**, 189 (1994).
[11] V. Cvetkovic and G. Dagan, ''Reactive transport and immiscible flow in geological media. Two applications,'' Proc. R. Soc. London, Ser. A **452**, 303 (1996).
[12] V. Cvetkovic, G. Dagan, and H. Cheng, ''Contaminant transport in aquifers with spatially variable flow and sorption properties,'' Proc. R. Soc. London, Ser. A **454**, 2173 (1998).
[13] G. Dagan and V. Cvetkovic, ''Reactive transport and immiscible flow in geological media 1. General theory,'' Proc. R. Soc. London, Ser. A **452**, 285 (1996).
[14] G. Dagan, ''Solute transport in heterogeneous porous formations,'' J. Fluid Mech. **145**, 151 (1984).
[15] G. Dagan, *Flow and Transport in Porous Formations* (Springer-Verlag, New York, 1989).
[16] M. L. Brusseau and P. S. C. Rao, ''Sorption nonideality during organic contaminant transport in porous media,'' CRC Crit. Rev. Environ. Control **19**, 33 (1989).
[17] J. N. Ryan and M. Elimelech, ''Colloid mobilization and transport in groundwater,'' Colloids Surf., A **107**, 1 (1996).

[18]J. N. Ryan and P. H. Gschwend, ''Colloid mobilization in two Atlantic coastal plain aquifers: Field studies,'' Water Resour. Res. **26**, 307 (1990).
[19]P. R. Johnson, N. Sun, and M. Elimelech, ''Colloid transport in geochemically heterogeneous porous media: Modeling and measurements,'' Environ. Sci. Technol. **30**, 3284 (1996).
[20]M. L. Brusseau, ''Transport of reactive contaminants in heterogeneous porous media,'' Rev. Geophys. **32**, 285 (1994).
[21]W. W. Wood, T. F. Kraemer, and P. P. Hearn, ''Intragranular diffusion: An important mechanism influencing solute transport in clastic aquifers?'' Science **247**, 1569 (1990).
[22]J. Villermaux, ''Deformation of chromatographic peaks under the influence of mass transfer phenomena,'' J. Chromatogr. **12**, 822 (1974).
[23]J. van der Lee, E. Ledoux, G. de Marsily, A. Vinsot, H. van de Weerd, A. Leijnse, B. Harmand, E. Rodier, M. Sardin, J. Dodds, and A. Hernandez Benitez, ''Development of a model for radionuclide transport by colloids in the biosphere,'' Final report EUR 17480 EN, European Commission, Luxemburg, 1997.
[24]G. Demmy, S. Berglund, and W. Graham, ''Injection mode implications for solute transport in porous media: Analysis in a stochastic Lagrangian framework,'' Water Resour. Res. **35**, 1965 (1999).
[25]R. Andricevic and V. Cvetkovic, ''Relative dispersion for solute flux in aquifers,'' J. Fluid Mech. **361**, 145 (1998).
[26]G. G. Demmy, ''Solute transport in heterogeneous porous formations,'' Ph.D. thesis, University of Florida, 1999.
[27]Special issue on nuclear waste, Phys. Today, Vol. 5, 1997.
[28]S. Painter, D. Turner, and V. Cvetkovic, ''Radionuclide retardation in the alluvial aquifer near Yucca Mountain, Nevada,'' Ground Water (in press).
[29]A. M. Shapiro and V. Cvetkovic, ''Stochastic analysis of solute arrival time in heterogeneous porous media,'' Water Resour. Res. **24**, 1711 (1988).
[30]Civilian Radioactive Waste Management System, Management and Operations, Total system assessment-Viability assessment (TSPA-VA) analyses. B00000000-01717-4301, Rev:01, CRWMS M&O, Las Vegas, Nevada, 1998.
[31]NRC sensitivity and uncertainty analyses for a proposed HLW repository at Yucca Mountain, Nevada using TPA 3.1: Results and conclusions. U.S. Nuclear Regulatory Commission, NUREG-1668, Vol. 2, Washington, DC, 1999.
[32]R. C. Thompson, ''Neptunium—the neglected actinide: A review of the biological and environmental literature,'' Radiat. Res. **90**, 1 (1982).
[33]D. R. Turner and R. T. Pabalan, ''Abstraction of mechanistic sorption model results for performance assessment calculations at Yucca Mountain, Nevada,'' Waste Management **19**, 375 (1999).
[34]P. Carbol and I. Engkvist, ''Compilation of radionuclide sorption coefficients for performance assessment,'' SKB Report R-97 13, Swedish Nuclear Fuel and Waste Management Co. (SKB), 1997.
[35]R. Andricevic and V. Cvetkovic, ''Evaluation of risk from contaminants migrating by groundwater,'' Water Resour. Res. **32**, 611 (1996).
[36]G. Destouni and W. Graham, ''Solute transport through an integrated soil-groundwater system,'' Water Resour. Res. **31**, 1935 (1995).
[37]G. Dagan and A. Fiori, ''The influence of pore-scale dispersion on concentration statistical moments in transport through heterogeneous aquifers,'' Water Resour. Res. **33**, 1595 (1997).
[38]A. Fiori, S. Berglund, V. Cvetkovic, and G. Dagan, ''Statistics of reactive solute flux in aquifers: Combined effect of pore-scale dispersion and sampling'' (unpublished).
[39]Y. Rubin, ''Stochastic modeling of macrodispersion in heterogeneous porous media,'' Water Resour. Res. **26**, 133 (1990).
[40]A. Bellin, P. Saladin, and A. Rinaldo, ''Simulation of dispersion in heterogeneous porous formations: Statistics, first-order theories, convergence of computations,'' Water Resour. Res. **28**, 2211 (1992).
[41]G. I. Taylor, ''Diffusion by continuous movements,'' Proc. London Math. Soc. **20**, 196 (1921).